Volume 1, Number 4

JPCR | JOURNAL OF PEDIATRIC CASE REPORTS

A MULTIDISCIPLINARY JOURNAL OF CASE REPORTS

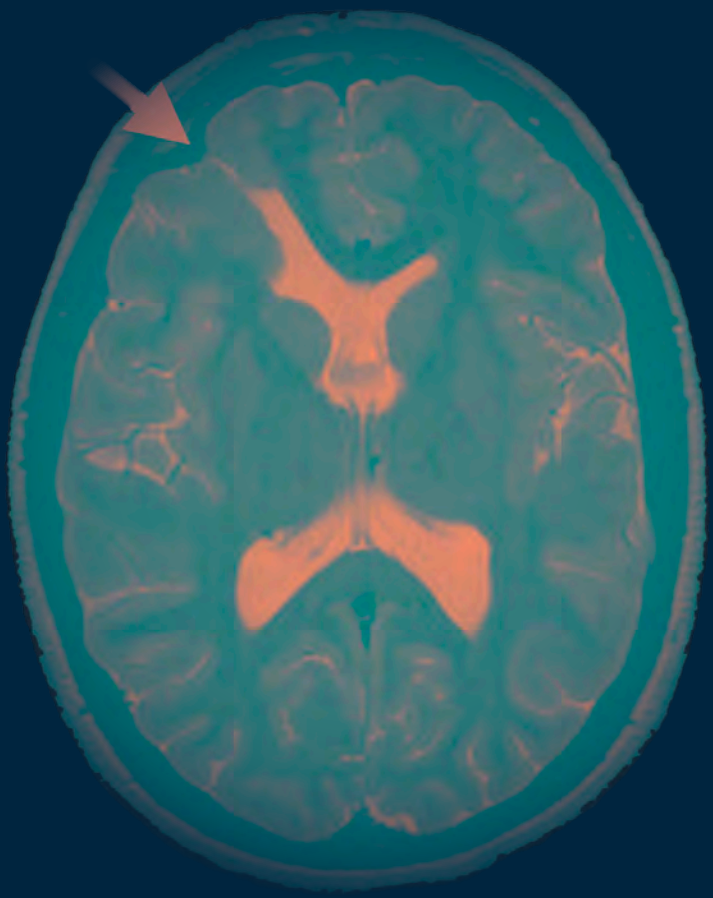

Stress Fractures in Children

Schizencephaly

Lymphangioleiomyomatosis

Gastroschisis

Congenital Nasal Pyriform Aperture Stenosis

Atrial Septal Defect

www.journalofpediatriccasereports.com

JPCR | JOURNAL OF PEDIATRIC CASE REPORTS

A MULTIDISCIPLINARY JOURNAL OF CASE REPORTS

Anderson Publishing, Ltd
180 Glenside Avenue,
Scotch Plains, NJ 07076
Tel: 908-271-8644

VOLUME 1 NUMBER 4

Stress Fractures in Children

Adrienne T. Ly, BA; Richard B. Towbin, MD; Carrie M. Schaefer, MD; Alexander J. Towbin, MD

Abstract

Stress fractures are microscopic disruptions of bone integrity that can occur in both children and adults. In pediatric patients, these injuries most commonly affect the lower extremities, particularly the tibia and metatarsals. Children involved in high-impact, running-intensive sports are at increased risk. Diagnosis can be challenging, as the microscopic nature of stress fractures makes them difficult to detect on radiographs. Advanced imaging modalities such as MRI and bone scintigraphy offer greater sensitivity for early detection. Because stress fractures typically do not result in displacement, treatment is generally conservative and includes activity modification, rest, and, in some cases, immobilization.

Keywords: musculoskeletal, lower extremity, trauma

Case Summary

An adolescent male high-jumper presented with worsening bilateral lower leg pain.

Imaging Findings

Initial radiograph of the left lower leg (Figure 1) was normal. MRI performed 5 days later (Figure 2) demonstrated edema-like signal in the medial proximal tibial metaphyses bilaterally. A discrete fracture line was visible on the left but not on the right. Follow-up radiograph performed 1 month later (Figure 3) showed healing changes at the site of the left tibial stress fracture.

Diagnosis

Stress fracture.

Differential diagnoses usually are pain related to repetitive activities or in children with a variety of conditions that result in decreased mineralization. Common repetitive activities resulting in pain in children include repeated running, jumping, throwing, or falling. Meanwhile, etiologies of decreased mineralization in children include genetically inherited osteogenesis imperfecta, rickets due to long-term vitamin D deficiency, or osteomyelitis.

Discussion

Stress fractures are microscopic cracks within bone, resulting from repetitive mechanical stress or reduced bone strength. Unlike complete fractures, stress fractures are incomplete and do not extend through the full thickness of the bone. They are broadly classified into 2 categories: fatigue fractures and insufficiency fractures. Fatigue fractures result from repeated mechanical loading that exceeds the bone's capacity for repair, commonly seen in athletes involved in repetitive high-impact activities.[1,2] In contrast, insufficiency fractures occur when normal stress is applied to weakened bone, such as in children with vitamin D deficiency or underlying metabolic bone disease.[1,3]

Figure 1. Anteroposterior radiograph of the proximal left tibia is normal.

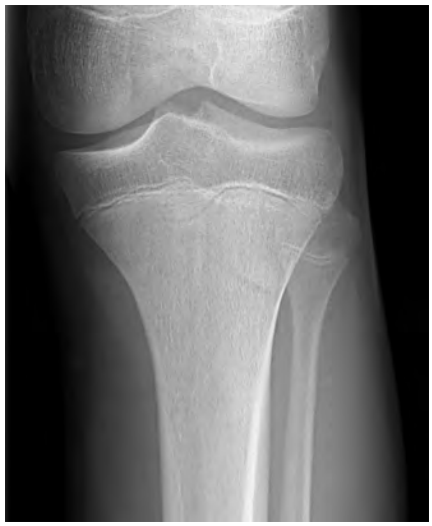

Stress fractures in children most commonly affect the lower extremities. In a retrospective analysis of pediatric lower extremity stress fractures, 28.4% were in the tibia, 24.1% in the metatarsals, 20.7% in the cuboid, 8.6% in the femur, 7.8% in the fibula, 6.9% in the calcaneus, and 3.4% in the cuneiform bones.[2] Stress fractures of the foot are frequently associated with long-distance running and high-impact sports such as basketball and soccer.[4] The

Affiliations: University of Arizona College of Medicine, Phoenix, Arizona (Ly); Department of Radiology, Phoenix Children's Hospital, Phoenix, Arizona (RB Towbin, Schaefer); Department of Radiology, Cincinnati Children's Hospital, University of Cincinnati College of Medicine, Cincinnati, Ohio (A Towbin).

Disclosures: The authors have no conflicts of interest to disclose. None of the authors received outside funding for the production of this original manuscript and no part of this article has been previously published elsewhere.

https://doi.org/10.37549/JPCR-26-0096

Figure 2. MRI performed 5 days after the initial radiograph. (A) Coronal STIR sequence of the lower legs showing edema signal within the medial aspect of each proximal tibial metaphysis. (A) T2 hypointense fracture line (arrow) is present on the left. The periosteum (arrowhead) is uplifted at the site of stress fracture. (B) Coronal T1-weighted image of the proximal left tibia showing amorphous low signal in the proximal tibia metaphysis. The periosteum (arrowhead) is uplifted at this location.

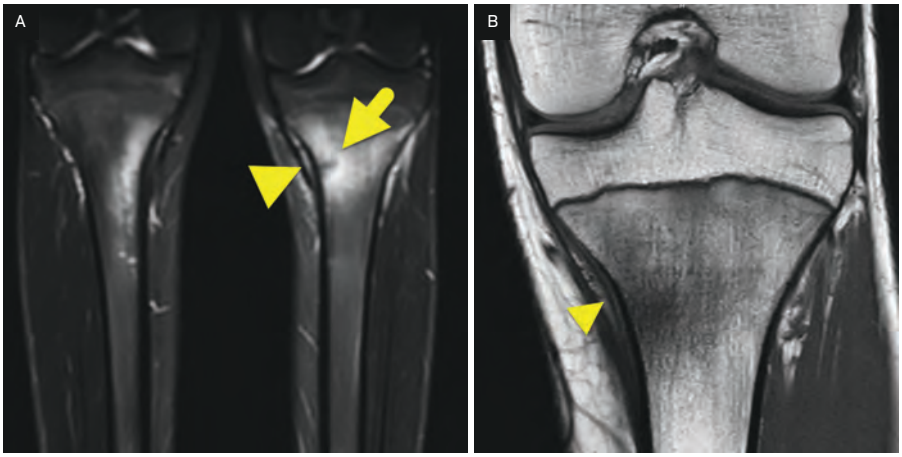

Figure 3. (A) Anteroposterior and (B) lateral radiographs performed 1 month later showing healing changes at the site of stress fracture with a linear band of sclerosis (arrow) and a healing periosteal reaction.

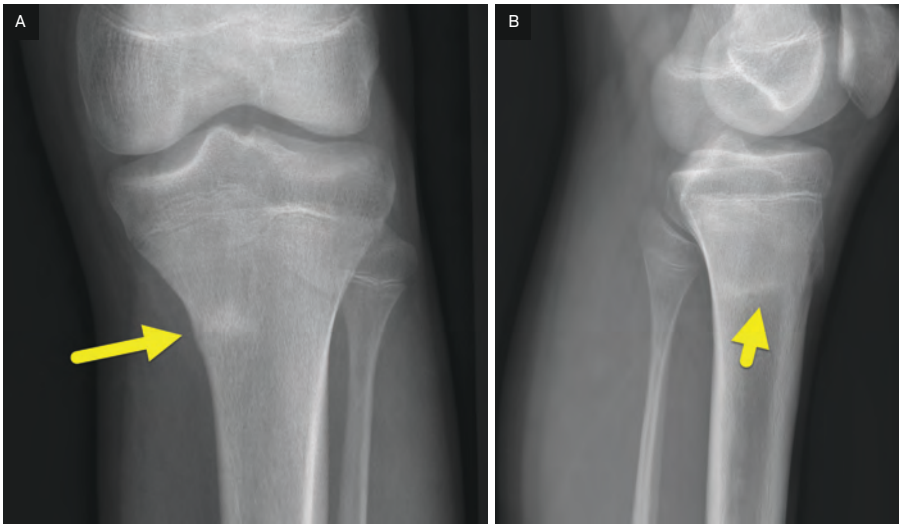

metatarsals are particularly vulnerable because they bear significant stress during the push-off phase of running.[4] Similarly, the tibia, fibula, and femur, as major weight-bearing bones, are at increased risk in children participating in high-impact activities like running and jumping.[4]

Although less common, stress fractures can also occur in the upper extremities. Examples include "little leaguer's shoulder," which involves the proximal humeral physis due to repetitive overhead throwing, and "gymnast's wrist," which affects the radial and/or ulnar physis from repetitive loading.[5] Additionally, stress fractures have been reported in the posterior column of the spine in young athletes performing repetitive spinning movements, such as figure skaters.[6]

On physical examination, stress fractures typically present with localized pain and guarding at the site of injury.[7] Because stress fractures do not cause displacement or angulation of the affected bone, skeletal deformity is not seen. Pain usually worsens with activity and improves with rest.[2] Soft tissue swelling near the fracture site may also be present.

Stress fractures can be challenging to diagnose radiographically, as fracture lines may not become visible until approximately 2 weeks after injury. Early radiographs have a sensitivity of only 15-35%, whereas MRI approaches nearly 100% sensitivity for detecting early-stage stress fractures.[1] When present, key radiographic findings include subtle lucency at the fracture site, trabecular blurring, and linear sclerosis.[1]

Advanced imaging techniques such as bone scintigraphy and MRI can improve early detection. A technetium-99m MDP bone scan can identify osseous injury 1-2 weeks earlier than radiographs.[8] On bone scintigraphy, areas of increased cortical uptake appear as hot spots, indicating osseous remodeling.[8] MRI findings include periosteal or adjacent soft tissue edema and band-like bone marrow edema.[1,3] A fracture line, when visible, appears as a hypointense band on T1-weighted sequences.[1]

The Fredericson grading system can be used to classify the severity of stress fractures on MRI, although the grading does not correlate with recovery time and is primarily used for documentation purposes.[9] The system ranges from grade 0 to grade 4b, as follows:

- **Grade 0**: normal.
- **Grade 1**: periosteal edema only, no bone marrow involvement.
- **Grade 2**: periosteal edema with bone marrow edema on T2-weighted imaging.
- **Grade 3**: periosteal edema with bone marrow edema visible on both T1- and T2-weighted imaging.
- **Grade 4a**: multiple focal intracortical signal abnormalities with bone marrow edema on T1 and T2.
- **Grade 4b**: linear intracortical signal abnormality with bone marrow edema on T1 and T2.

Because stress fractures are incomplete and cause minimal displacement, initial management is typically conservative. Treatment includes activity modification, rest, and physical therapy focused on stretching and strengthening the surrounding muscles.[7,10] If needed, immobilization with a cast for 3-6 weeks can be considered.[7] Surgical fixation with intramedullary nails or screws is reserved for high-risk fractures that may progress to complete fractures.[2]

Healing usually takes about 6-8 weeks, though recovery time varies depending on fracture location and treatment approach. Stress fractures in cortical-rich regions, such as long bone shafts, tend to heal faster than those in trabecular-rich areas, such as the epiphyseal ends.[3] Recovery time is typically longer when surgical intervention is required.[2] In one study, pediatric patients returned to activity at an average of 11.4 weeks, with recovery times ranging from 4.5 to 17.4 weeks.[2]

Conclusion

Stress fractures are microscopic disruptions of bone integrity that can occur in both children and adults. In pediatric patients, these injuries most commonly affect the lower extremities, particularly the tibia and metatarsals. Children involved in high-impact, running-intensive sports are at increased risk. Diagnosis can be challenging, as the microscopic nature of stress fractures makes them difficult to detect on radiographs. Advanced imaging modalities such as MRI and bone scintigraphy offer greater sensitivity for early detection. Because stress fractures typically do not result in displacement, treatment is generally conservative and includes activity modification, rest, and, in some cases, immobilization.

References

1) Marshall RA, Mandell JC, Weaver MJ, et al. Imaging features and management of stress, atypical, and pathologic fractures. *Radiographics*. 2018;38(7):2173-2192. doi:10.1148/rg.2018180073

2) Gremillion MJ, Martinez A, Ghanta RB, Borici N, Kushare I. An assessment of the diagnosis, treatment, and outcomes of lower extremity stress fractures in pediatric and adolescent populations. *Phys Sportsmed*. 2023;51(6):572-581. doi:10.1080/00913847.2022.2143247

3) Armento A, Heronemus M, Truong D, Swanson C. Bone health in young athletes: a narrative review of the recent literature. *Curr Osteoporos Rep*. 2023;21(4):447-458. doi:10.1007/s11914-023-00796-5

4) Strassberg J, Ahmed A. Pediatric sports injuries. *Clin Podiatr Med Surg*. 2022;39(1):89-103. doi:10.1016/j.cpm.2021.08.003

5) Kim HHR, Menashe SJ, Ngo A-V, et al. Uniquely pediatric upper extremity injuries. *Clin Imaging*. 2021;80:249-261. doi:10.1016/j.clinimag.2021.07.010

6) Kowalczyk AD, Geminiani ET, Dahlberg BW, Micheli LJ, Sugimoto D. Pediatric and adolescent figure skating injuries: a 15-year retrospective review. *Clin J Sport Med*. 2021;31(3):295-303. doi:10.1097/JSM.0000000000000743

7) Grossman J, Giliberti B, Dolitsky R, et al. Pediatric orthopedic trauma. *Pediatr Clin North Am*. 2020;67(1):101-118. doi:10.1016/j.pcl.2019.09.010

8) Serino J, Kunze KN, Jacobsen SK, et al. Nuclear medicine for the orthopedic foot and ankle surgeon. *Foot Ankle Int*. 2020;41(5):612-623. doi:10.1177/1071100720910422

9) Ditmars FS, Ruess L, Young CM, et al. MRI of tibial stress fractures: relationship between fredericson classification and time to recovery in pediatric athletes. *Pediatr Radiol*. 2020;50(12):1735-1741. doi:10.1007/s00247-020-04760-8

10) Farrell C, Hannon M, Monuteaux MC, Mannix R, Lee LK. Pediatric fracture epidemiology and US emergency department resource utilization. *Pediatr Emerg Care*. 2022;38(7):e1342-e1347. doi:10.1097/PEC.0000000000002752

https://doi.org/10.37549/JPCR-26-0096

Schizencephaly

Alyssa H. Sze, MS; Richard B. Towbin, MD; Carrie M. Schaefer, MD; Alexander J. Towbin, MD

Abstract

Schizencephaly is a rare cortical malformation characterized by a full-thickness gray matter-lined cleft extending from the pial surface to the ventricular wall. This defect is frequently associated with other intracranial abnormalities, including absence of the septum pellucidum, optic nerve hypoplasia, corpus callosum dysplasia, hydrocephalus, arachnoid cysts, and cerebellar malformations. While increasingly diagnosed antenatally, many patients present later in life with seizures, intellectual disability, or psychomotor delay. Clinical severity is closely related to the size and location of the cleft. Management is symptom-based and may include medical treatment for seizures, shunt placement for hydrocephalus, and supportive therapies for developmental and motor impairments.

Keywords: brain, congenital, genetic

Case Summary

An adolescent, who was a restrained passenger in a motor vehicle collision, presented to the emergency department following a brief loss of consciousness. On examination, her Glasgow Coma Scale score was 15. Notably, the patient did not have a history of seizures.

Imaging Findings

Initial head CT (Figure 1) showed no traumatic findings. Instead, the study showed the absence of the septum pellucidum, closed-lip schizencephaly in the inferior right frontal lobe with mild distortion of the adjacent lateral ventricle, and closed-lip schizencephaly and polymicrogyria in the left frontal lobe. Subsequent MRI (Figure 2) confirmed these findings.

Figure 1. Axial CT images at the level of (A) the frontal horns of the lateral ventricles and (B) the body of the lateral ventricles showing the absence of the septum pellucidum and bilateral closed-lip schizencephaly (arrow) with gray matter lining each cleft.

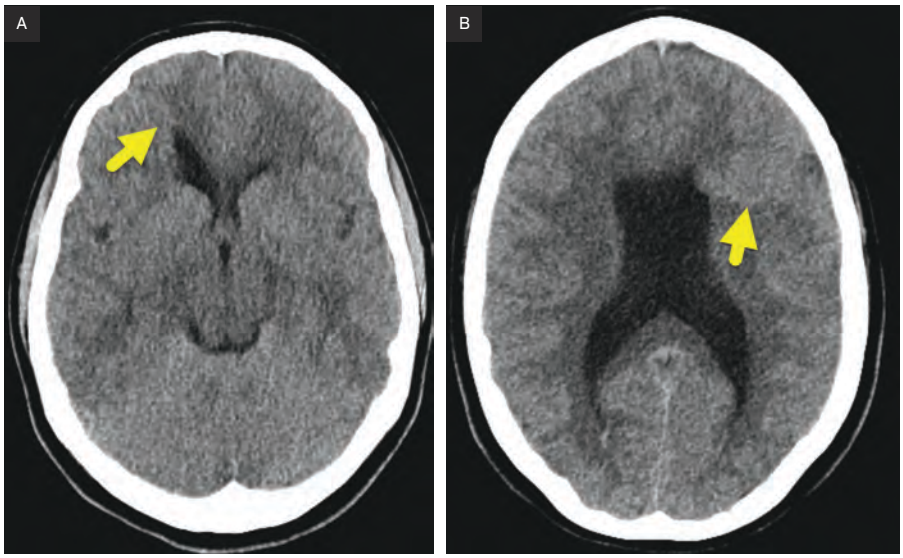

Diagnosis

Schizencephaly.

The imaging differential diagnosis for schizencephaly includes porencephaly, heterotopic gray matter, gliosis, focal cortical dysplasia, polymicroglia, arachnoid cysts, and septo-optic dysplasia.

Discussion

Schizencephaly is a rare malformation of the cerebral cortex occurring with a prevalence of 1.54 per 100,000

Affiliations: Virginia Tech Carilion School of Medicine, Roanoke, Virginia (Sze); Department of Radiology, Phoenix Children's Hospital, Phoenix, Arizona (RB Towbin, Schaefer); Department of Radiology, Cincinnati Children's Hospital, University of Cincinnati College of Medicine, Cincinnati, Ohio (AJ Towbin).
Disclosures: The authors have no conflicts of interest to disclose. None of the authors received outside funding for the production of this original manuscript and no part of this article has been previously published elsewhere.

https://doi.org/10.37549/JPCR-26-0097

Figure 2. (A) Axial T2-weighted and (B) T1 FLAIR images at the level of the frontal horns of the lateral ventricles and (C) axial T2-weighted and (D) T1 FLAIR images at the level of the mid body of the lateral ventricles showing the absence of the septum pellucidum and bilateral closed-lip schizencephaly (arrow) with gray matter lining each cleft. Polymicrogyria is present at each cleft.

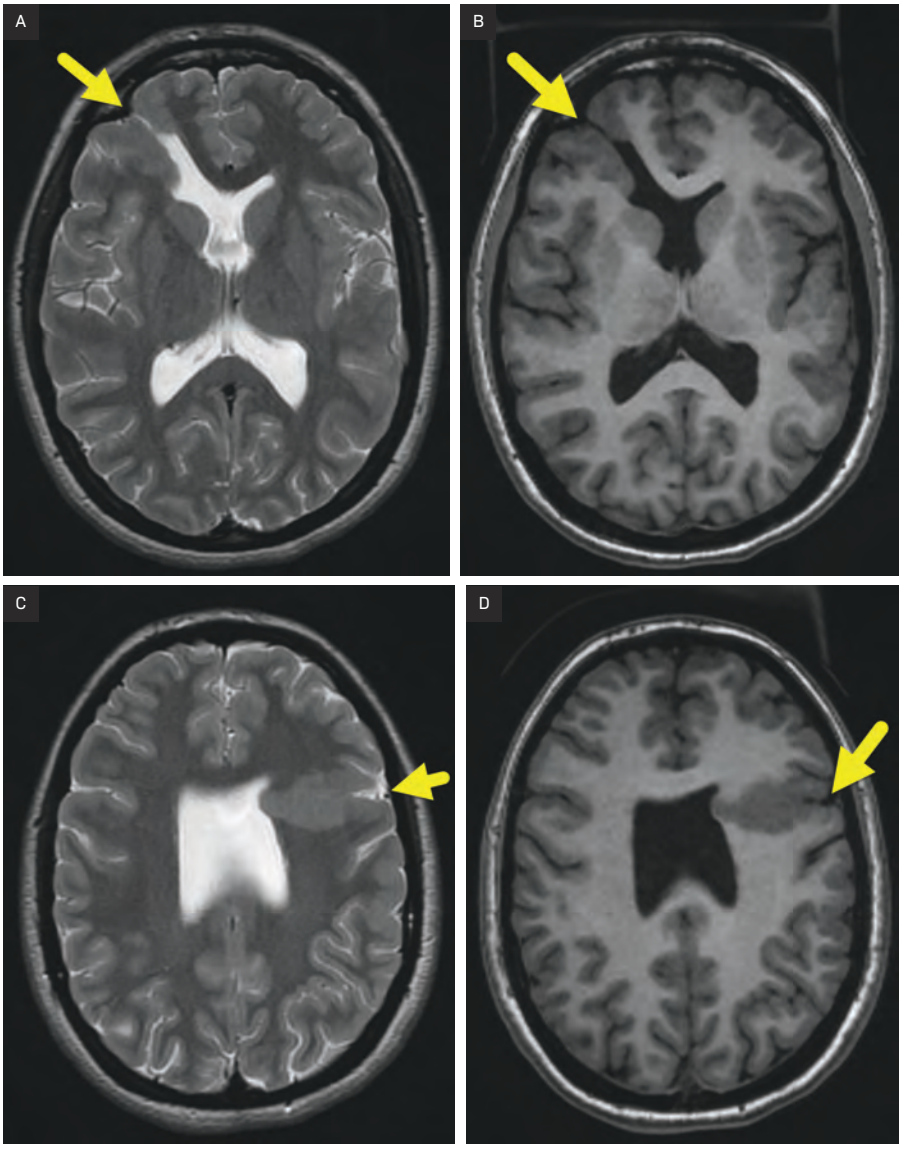

births.[1] It is characterized by a full-thickness gray matter-lined cleft that extends from the pial surface to the ventricular wall. The cleft's gray matter lining distinguishes it from other cortical abnormalities.[2] Schizencephaly typically occurs sporadically. Only a few familial cases have been described.[3] However, it has been occasionally associated with mutations in the *EMX2* and *COL4A1* genes, as well as with Vici syndrome, a disorder caused by *EPG5* gene mutations and characterized by agenesis of the corpus callosum, cardiomyopathy, albinism, and immune deficiency.

The etiology of schizencephaly remains unclear. Proposed mechanisms include intrauterine infections and early vascular disruptions.[1] One hypothesis suggests that intracranial insults occurring before neuronal migration (4-6 months gestational age) result in schizencephaly, while injuries after this period produce defects not lined by gray matter, such as porencephaly (without gliosis) or encephalomalacia (with gliosis).[4] Additional risk factors include young maternal age (under 20 years), prenatal exposure to toxins or teratogens, and maternal trauma.[3]

Schizencephaly can be distinguished from other intracranial abnormalities, such as porencephaly, by the presence of a gray matter lining along the cleft. Porencephaly refers to a cystic cavity within the cerebral hemisphere that communicates with the ventricular system or subarachnoid space. These cavities are typically surrounded by gliosis, lack a gray matter lining, and are usually the result of acquired brain injury. While antenatal US is increasingly capable of detecting schizencephaly in utero, MRI remains the preferred imaging modality due to its ability to clearly visualize the gray matter lining.[3]

Schizencephaly is typically classified into 2 types: type 1 (closed-lip) and type 2 (open-lip). In open-lip schizencephaly, the cleft walls are separated and filled with cerebrospinal fluid. In contrast, closed-lip schizencephaly is characterized by direct apposition of the cleft walls without intervening fluid. More recent literature proposes an expanded classification that includes a third variant: a column of heterotopic gray matter without a visible cleft. In this system, type 1 represents isolated gray matter heterotopia, type 2 corresponds to closed-lip schizencephaly, and type 3 to open-lip schizencephaly.[1,4]

Open-lip schizencephaly is the most common form, seen in approximately 80-85% of patients, while closed-lip accounts for the remaining 10-15%. Schizencephaly may be unilateral or bilateral, with bilateral involvement slightly more frequent. Among patients with bilateral clefts, 60% have bilateral open-lip defects, and 20% have mixed defects. Of those with unilateral clefts, 60% have open-lip defects.[4]

Between 50% and 90% of patients with schizencephaly have additional intracranial anomalies. The most common

associated abnormality is absence of the septum pellucidum, seen in approximately 70% of patients. Other frequent findings include optic nerve hypoplasia (30%), corpus callosum dysplasia (30%), and hydrocephalus, which occurs in about 30% of patients with open-lip clefts.[3-5] Additional associations include arachnoid cysts and cerebellar malformations.[3]

When schizencephaly is not detected on antenatal imaging, it is often identified later in childhood during evaluation for psychomotor delay or seizures. In patients with a unilateral cleft, seizures may originate from the contralateral hemisphere, often in regions of polymicrogyria.[5] The severity of symptoms and overall prognosis correlates with the size and location of the cleft. Larger or bilateral defects are associated with more significant motor and cognitive impairments, including hemiparesis or quadriparesis, intellectual disability, language deficits, and global developmental delay.[1,6] Frontal or perisylvian clefts may also be associated with behavioral disturbances or characteropathies.[3]

In contrast, unilateral schizencephaly may be asymptomatic and is sometimes discovered incidentally in adulthood, often after the onset of seizures in individuals with otherwise normal development.[7] Treatment is symptom-directed and may include antiepileptic medications, ventriculoperitoneal shunting for hydrocephalus, and supportive therapies such as occupational and physical therapy to address cognitive and motor impairments.[1,8]

Conclusion

Schizencephaly is a rare cortical malformation characterized by a full-thickness gray matter-lined cleft extending from the pial surface to the ventricular wall. This defect is frequently associated with other intracranial abnormalities, including the absence of the septum pellucidum, optic nerve hypoplasia, corpus callosum dysplasia, hydrocephalus, arachnoid cysts, and cerebellar malformations. While increasingly diagnosed antenatally, many patients present later in life with seizures, intellectual disability, or psychomotor delay. Clinical severity is closely related to the size and location of the cleft. Management is symptom-based and may include medical treatment for seizures, shunt placement for hydrocephalus, and supportive therapies for developmental and motor impairments.

References

1) Hashim HT, Ahmad MS, Gataa IS. Schizencephaly. In: AlAli KF, Hashim HT, eds. *Congenital Brain Malformations*. Springer. 2024. doi:10.1007/978-3-031-58630-9_14

2) Oh KY, Kennedy AM, Frias AE Jr, Byrne JLB. Fetal schizencephaly: pre- and postnatal imaging with a review of the clinical manifestations. *Radiographics*. 2005;25(3):647-657. doi:10.1148/rg.253045103

3) Halabuda A, Klasa L, Kwiatkowski S, et al. Schizencephaly-diagnostics and clinical dilemmas. *Childs Nerv Syst*. 2015;31(4):551-556. doi:10.1007/s00381-015-2638-1

4) Griffiths PD. Schizencephaly revisited. *Neuroradiology*. 2018;60(9):945-960. doi:10.1007/s00234-018-2056-7

5) Naidich TP, Griffiths PD, Rosenbloom L. Central nervous system injury in utero: selected entities. *Pediatr Radiol*. 2015;45(s3):S454-62. doi:10.1007/s00247-015-3344-6

6) Hung P-C, Wang H-S, Chou M-L, et al. Schizencephaly in children: a single medical center retrospective study. *Pediatr Neonatol*. 2018;59(6):573-580. doi:10.1016/j.pedneo.2018.01.009

7) Paudel K, Prasad T, Gyawali P, Nepal G, Jaiswal V. Schizencephaly diagnosed after an episode of seizure during labor: a case report. *Clin Case Rep*. 2023;11(5):e7328. doi:10.1002/ccr3.7328

8) Ghosn Y, Kamareddine MH, Adem C, Jabbour R. A patient with schizencephaly and agenesis of corpus callosum with no neurological deficits. *J Neurosci Rural Pract*. 2018;9(3):404-405. doi:10.4103/jnrp.jnrp_564_17

https://doi.org/10.37549/JPCR-26-0097

Lymphangioleiomyomatosis

Tal A. Chamdi, BS; Richard B. Towbin, MD; Carrie M. Schaefer, MD; Alexander J. Towbin, MD

Abstract

Although the diagnosis of tuberous sclerosis complex-lymphangioleiomyomatosis (TSC-LAM) is rare in adolescents, emerging data suggest that its true incidence, particularly among females with TSC, may be underestimated. High-resolution CT of the chest is critical for identifying characteristic pulmonary cysts, while abdominal imaging plays a supportive role by detecting associated renal angiomyolipomas. Given the progressive nature of LAM, early recognition is essential for guiding management and improving outcomes. Clinicians should maintain a high index of suspicion for LAM in adolescents with TSC2 gene mutations.

Keywords: pulmonary, lung, congenital

Case Summary

An adolescent female with tuberous sclerosis complex (TSC) underwent screening chest CT.

Imaging Findings

Initial chest CT (Figure 1) demonstrated multiple small, thin-walled cysts predominantly located in the right lower lobe, consistent with early findings of lymphangioleiomyomatosis (LAM). Follow-up chest CT (Figure 2) performed 12 years later showed mild progression in the number and size of pulmonary cysts. Abdominal MRI (Figure 3) revealed multiple renal angiomyolipomas (AMLs), most of which were lipid-poor. The largest lesion was in the lower pole of the right kidney.

Diagnosis

TSC-LAM.

Differential diagnosis includes sporadic LAM, emphysema, Sjögren syndrome, pulmonary Langerhans cell histiocytosis, follicular bronchiolitis, lymphoid interstitial pneumonia, amyloidosis, light-chain deposition disease, and Birt-Hogg-Dube syndrome.

Discussion

LAM is a rare, progressive multisystem disease that primarily affects women of childbearing age, with an estimated prevalence of 3.4-7.8 per million women worldwide.[1] It is characterized by the proliferation of abnormal smooth muscle—like cells that infiltrate the lungs and lymphatics, leading to progressive cystic destruction, impaired pulmonary function, and, ultimately, respiratory failure.[2]

LAM occurs in 2 forms: a sporadic form, which typically presents in adulthood, and a form associated with TSC, which may present in childhood.[2] TSC-LAM is increasingly recognized as a significant cause of morbidity in women with TSC. Among adult women with TSC, approximately 30-40% will develop LAM. The condition is significantly more common in those with TSC2 mutations than in those with TSC1 mutations, with one study reporting a prevalence of 55% vs 0%, respectively.[3] Serum VEGF-D levels are also typically higher in patients with LAM and TSC2 mutations and may serve as a useful biomarker for the presence of LAM.[3] In a study by Cudzilo et al, the prevalence of LAM in females under the age of 21 with TSC was 27%, suggesting that disease onset may occur earlier than previously recognized.[4] Another study showed that lung cysts were present in 12% of patients with TSC who had received a chest CT, including 20% of women.[5] Nevertheless, diagnosis in adolescents remains rare, likely due to a combination of factors, including the absence of respiratory symptoms, lack of universal screening protocols in the pediatric populations, and the subtle, nonspecific appearance of early pulmonary changes on imaging.[4,6]

In adolescents, TSC-LAM is often asymptomatic, but when symptoms do occur, they may include exertional dyspnea or spontaneous pneumothorax. Imaging, chest CT, plays a central role in diagnosis. According to the 2017 American Thoracic Society/Japanese Respiratory Society guidelines, LAM can be diagnosed

Affiliations: Central Michigan University, College of Medicine, Mount Pleasant, Michigan (Chamdi); Phoenix Children's Hospital, Phoenix, Arizona (RB Towbin, Schaefer); Cincinnati Children's Hospital, Cincinnati College of Medicine, Cincinnati, Ohio (AJ Towbin).
Disclosures: The authors have no conflicts of interest to disclose. None of the authors received outside funding for the production of this original manuscript and no part of this article has been previously published elsewhere.

https://doi.org/10.37549/JPCR-26-0098

Figure 1. (A, B) Sequential images from chest CT showing several small cysts (arrows) with imperceptible walls.

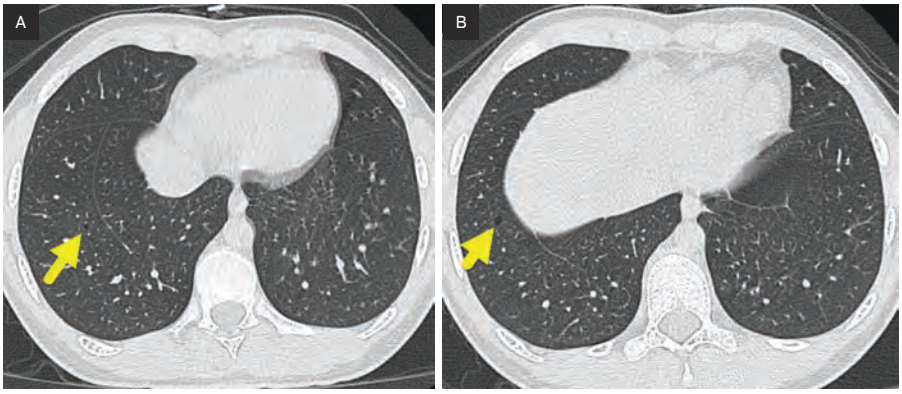

Figure 2. (A, B) Sequential images from chest CT performed 12 years later showing that the small cysts (arrow) have increased in size and number. (C, D) Minimum intensity projection images at the same levels highlighting the extent of the small cysts.

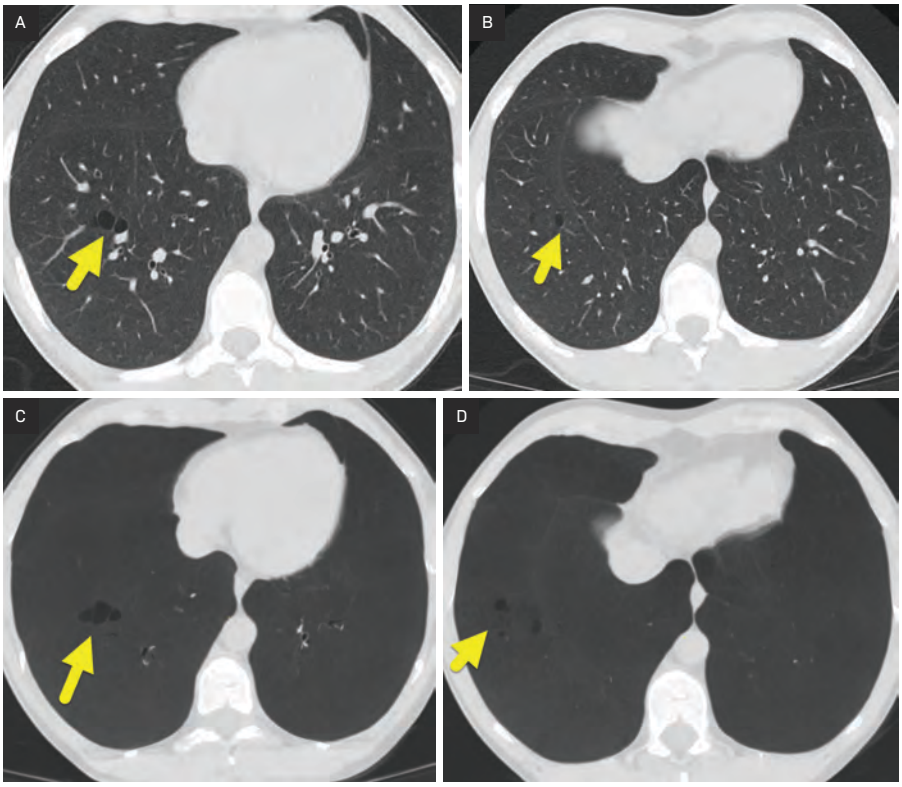

based on the presence of characteristic diffuse, thin-walled, round pulmonary cysts, in conjunction with one or more supportive features, such as TSC, renal AML, cystic lymphangioleiomyoma, chylothorax, or chylous ascites.[7]

Chest radiographic findings vary depending on disease severity: patients with early-stage disease may have a normal radiograph or may have mildly increased interstitial markings. Patients with advanced disease may demonstrate reticular opacities, pleural thickening, lymphadenopathy, and hyperinflation.[1,2]

Current TSC guidelines recommend baseline chest CT for all females and symptomatic males, starting at 18 years of age.[8] On chest CT, TSC-LAM is characterized by numerous thin-walled, round, or oval cysts distributed throughout the

Figure 3. Coronal T2-weighted MRI showing a dominant lipid-poor angiomyolipoma in the lower pole of the right kidney. There are many tiny angiomyolipomata throughout both kidneys, giving the cortex a striated appearance.

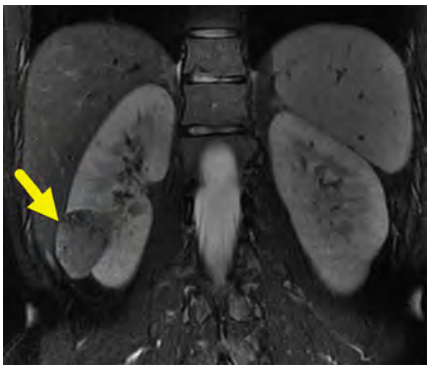

lungs.[1] In early disease, cysts are fewer and smaller, with intervening normal lung parenchyma. At this stage, the cysts may be more visible on minimum intensity projection images. As the disease progresses, cysts become more numerous and larger, gradually replacing healthy lung tissue. Additional CT findings may include focal ground-glass opacities, lymphatic congestion, septal thickening, chylothorax, pericardial effusion, and thoracic duct dilation.[1,2] TSC-LAM may also be associated with multifocal micronodular pneumocyte hyperplasia.[1] Certain imaging features help distinguish LAM from other diffuse cystic lung diseases. For example, thick, irregular upper lobe cysts are more typical of pulmonary Langerhans cell histiocytosis.[1]

Abdominal and pelvic imaging with CT or MRI is essential, as over 90% of patients with TSC-LAM and approximately one-third of those with sporadic LAM have renal AMLs.[9] On CT, AMLs typically involve the renal cortex and often contain macroscopic fat. However, in patients with TSC-LAM, up to one-third of AMLs may be fat-poor, making detection more challenging.[10] On MRI, classic AMLs demonstrate signal loss on fat-suppressed sequences. Chemical shift MRI can also detect small amounts of fat by revealing signal loss within voxels that contain both fat and water, often

producing an "India-ink" artifact at the fat-water interface of the lesion.[11]

Management of LAM focuses on alleviating symptoms and slowing disease progression. Recurrent or complicated pneumothoraces may be treated with pleurodesis, and lung transplantation is considered in patients with advanced respiratory failure. More recently, mTOR inhibitors such as sirolimus have emerged as a key therapy, shown to stabilize lung function and reduce the size of associated tumors in patients with LAM.[1,2]

Conclusion

Although the diagnosis of TSC-LAM is rare in adolescents, emerging data suggest that its true incidence, particularly among females with TSC, may be underestimated. High-resolution CT of the chest is critical for identifying characteristic pulmonary cysts, while abdominal imaging plays a supportive role by detecting associated renal AMLs. Given the progressive nature of LAM, early recognition is essential for guiding management and improving outcomes. Clinicians should maintain a high index of suspicion for LAM in adolescents with TSC2 gene mutations.

References

1) McCarthy C, Gupta N, Johnson SR, Yu JJ, McCormack FX. Lymphangioleiomyomatosis: pathogenesis, clinical features, diagnosis, and management. *Lancet Respir Med*. 2021;9(11):1313-1327. doi:10.1016/S2213-2600(21)00228-9

2) O'Mahony AM, Lynn E, Murphy DJ, Fabre A, McCarthy C. Lymphangioleiomyomatosis: a clinical review. *Breathe*. 2020;16(2):200007. doi:10.1183/20734735.0007-2020

3) Tian X, Glass JE, Kwiatkowski DJ, et al. Lymphangioleiomyomatosis association with underlying genotype in patients with tuberous sclerosis complex. *Ann Am Thorac Soc*. 2021;18(5):815-819. doi:10.1513/AnnalsATS.202008-911OC

4) Cudzilo CJ, Szczesniak RD, Brody AS, et al. Lymphangioleiomyomatosis screening in women with tuberous sclerosis. *Chest*. 2013;144(2):578-585. doi:10.1378/chest.12-2813

5) Ritter DM, Fessler BK, Ebrahimi-Fakhari D, et al. Prevalence of thoracoabdominal imaging findings in tuberous sclerosis complex. *Orphanet J Rare Dis*. 2022;17(1):124. doi:10.1186/s13023-022-02277-x

6) Johnson J, Somerfield W, Johnson SR. Lymphangioleiomyomatosis in patients with tuberous sclerosis: a national centre audit. *Orphanet J Rare Dis*. 2024;19(1):137. doi:10.1186/s13023-024-03115-y

7) McCormack FX, Gupta N, Finlay GR, et al. Official American thoracic society/Japanese respiratory society clinical practice guidelines: lymphangioleiomyomatosis diagnosis and management. *Am J Respir Crit Care Med*. 2016;194(6):748-761. doi:10.1164/rccm.201607-1384TH

8) Northrup H, Aronow ME, Bebin EM, et al. Updated international tuberous sclerosis complex diagnostic criteria and surveillance and management recommendations. *Pediatr Neurol*. 2021;123:50-66. doi:10.1016/j.pediatrneurol.2021.07.011

9) Avila NA, Dwyer AJ, Rabel A, Moss J. Sporadic lymphangioleiomyomatosis and tuberous sclerosis complex with lymphangioleiomyomatosis: comparison of CT features. *Radiology*. 2007;242(1):277-285. doi:10.1148/radiol.2421051767

10) Silverman SG, Israel GM, Herts BR, Richie JP. Management of the incidental renal mass. *Radiology*. 2008;249(1):16-31. doi:10.1148/radiol.2491070783

11) Thiravit S, Teerasamit W, Thiravit P. The different faces of renal angiomyolipomas on radiologic imaging: a pictorial review. *Br J Radiol*. 2018;91(1084):20170533. doi:10.1259/bjr.20170533

https://doi.org/10.37549/JPCR-26-0098

Gastroschisis

Priya Patel, BS; Richard B. Towbin, MD; Carrie M. Schaefer, MD; Alexander J. Towbin, MD

Abstract

An external protrusion of the intestines and occasionally other organs without a protective membrane is the hallmark of gastroschisis. Prenatal US, specifically the marker intraabdominal bowel distention, is the most effective in diagnosing and differentiating between simple and complex gastroschisis. Patients diagnosed with the condition are at a risk of infection, sepsis, and electrolyte imbalances from swelling and inflammation of the exposed organs. Treatment aims for primary reduction of the herniated viscera to prevent visceral injury and abdominal compartment syndrome. Staged reduction using a spring-loaded silo is the preferred method. Complex cases should be treated individually, and any resection should be kept to a minimum to prevent short-gut syndrome. Reported complications include abdominal compartment syndrome (up to 25%), necrotizing enterocolitis (5%), midgut volvulus (1.2%), and adhesive small bowel obstruction (20-25%).

Keywords: gastrointestinal, intestines, congenital

Case Summary

A mother with a history of cocaine use during pregnancy underwent detailed fetal US due to findings on screening US. The fetus was born at term via c-section and transferred to the neonatal intensive care unit.

Imaging Findings

Fetal US (Figure 1) showed gastroschisis with dilated loops of bowel, with thickened walls extending through a midline abdominal wall defect adjacent to the umbilical cord. Postnatal radiograph (Figure 2) showed eviscerated bowel loops external to the abdomen. Radiograph performed 2 hours later (Figure 3) showed the loops of bowel within an abdominal silo.

Diagnosis

Gastroschisis.

The differential diagnosis for an anterior abdominal wall defect with protrusion of organs outside of the fetus is an omphalocele.

Discussion

Gastroschisis is a full-thickness, congenital defect involving the anterior abdominal wall that occurs in utero and occurs in about 1/10,000 live births and is usually an isolated anomaly. Gastroschisis occurs between the 4 and 8 weeks of gestational age. The cause is unknown but suspected to be the result of compromised vascular supply. The uncovered intestine, and rarely other organs, herniates through the abdominal wall defect near the right base of the umbilical cord. Typically, >90% of cases are diagnosed on fetal ultrasonography at 20 weeks of gestational age.[1] Pregnancies complicated by gastroschisis have an increased risk of stillbirth, small for gestational age infants, necrotizing enterocolitis (NEC), and neonatal death. Depending on the state of the colon, there are 2 types of gastroschisis: simple and complex. The bowel is healthy in simple gastroschisis. In contrast, complex gastroschisis is associated with conditions such as volvulus, ischemia, atresia, or necrosis.[2]

Figure 1. Fetal US image showing dilated and mildly thickened loops of bowel (arrow) external to the abdomen (arrowhead).

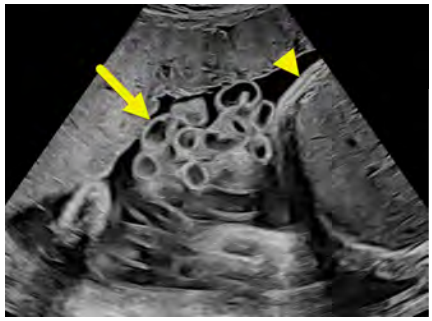

Affiliations: Burrell College of Osteopathic Medicine, Las Cruces, New Mexico (Patel); Department of Radiology, Phoenix Children's Hospital, Phoenix, Arizona (RB Towbin, Schaefer); Department of Radiology, Cincinnati Children's Hospital, University of Cincinnati College of Medicine, Cincinnati, Ohio (AJ Towbin).
Disclosures: The authors have no conflicts of interest to disclose. None of the authors received outside funding for the production of this original manuscript and no part of this article has been previously published elsewhere.

https://doi.org/10.37549/JPCR-26-0099

Figure 2. Abdominal radiograph showing eviscerated bowel (arrow) external to the abdomen.

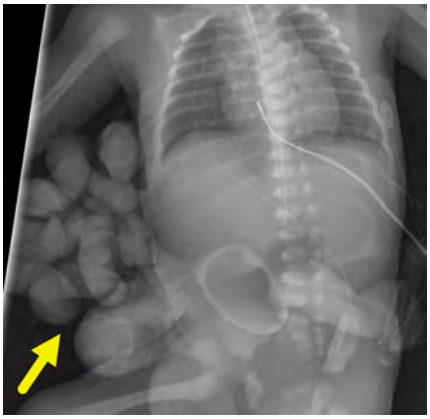

Figure 3. Abdominal radiograph performed 2 hours later showing the eviscerated bowel (arrow) within an abdominal silo.

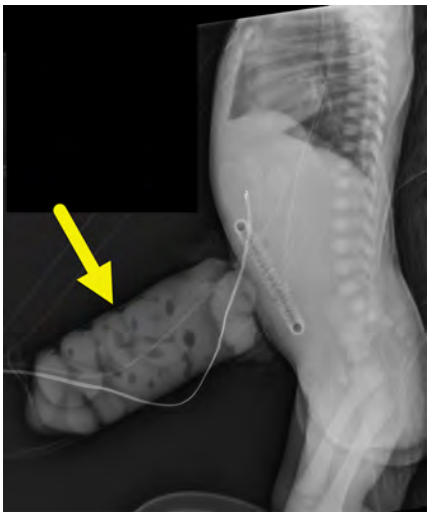

Although gastroschisis and omphalocele are both abdominal wall defects, their presentation has characteristic differences. Gastroschisis is an abdominal wall defect, most often to the right of the umbilicus. It is usually a solitary anomaly with post-delivery outcomes related to the prolapsed bowel. The prolapsed bowel lacks a covering membranous sac, and the intestines protrude outside the fetal abdomen into the amniotic cavity because of an in utero interruption of the lateral ventral body folds.[3] While gastroschisis is not associated with other congenital anomalies, it is commonly associated with bowel complications, which include malrotation (up to 25% of cases), intestinal atresia and stenosis (10% of cases), or NEC (5-20%) that further complicate the condition.[2]

Omphalocele is an abdominal wall defect that differs from gastroschisis due to its midline location and sac covering the herniated intestines. The abdominal wall defect in omphaloceles can vary in size. When small, only a portion of the intestines may herniate. When a large abdominal wall defect occurs, most abdominal organs can herniate. Omphaloceles are associated with genetic syndromes and anomalies that will determine the patient's outcome. Multiple congenital abnormalities are present in 40-80% of patients and include chromosomal (15-57%), cardiac (11-23%), genitourinary (6-21%), musculoskeletal (21%), gastrointestinal (7-19%), and neurologic (4-8%) issues.[3]

Fetal growth restriction occurs in 24-67% of fetuses with gastroschisis and is thought to be due to the nonselective loss of nutrients, mainly proteins, through the externalized bowel loops, causing chronic undernutrition of the fetus. This is supported by the fact that high levels of proteins are found in the amniotic fluid. In a recent meta-analysis, delivery at 38 weeks was found to minimize overall perinatal mortality and maximize total quality-adjusted life-years in fetuses with gastroschisis. Cesarean section was once thought by some to be the best delivery route for the fetus with gastroschisis because it reduced the risk of trauma to intestinal loops and avoided contact with vaginal flora.[4] However, based on current evidence, vaginal delivery for infants with gastroschisis has no contraindications based on factors such as timing (lung maturity), US findings (fetal growth, bowel appearance), and fetal testing results. Therefore, while the mean gestational age for spontaneous vaginal delivery is 36 weeks, delivery at 38 weeks of gestation is the preferred method for women carrying a fetus with gastroschisis to minimize complications. If there are associated complications, such as marked liver herniation, then cesarean section should be considered.[5]

At birth, neonates with gastroschisis may have hypothermia or intestines that appear discolored, suggesting injury or insufficient blood flow. Rarely, additional internal organs may herniate, including the pancreas, stomach, liver, spleen, bladder, uterus, ovaries, and fallopian tubes.[1] Neonates affected by this condition may also suffer from sepsis, NEC, short bowel syndrome, bowel obstruction, and volvulus.[4]

Prenatal US can diagnose gastroschisis as early as the first trimester. The prenatal US may show the herniated bowel floating in the amniotic fluid. Prenatal US can also provide prognostic information. Measurement of intra-abdominal bowel dilation at the most dilated bowel segment can distinguish complex from simple gastroschisis. A recent longitudinal, prospective multicenter study of 104 patients showed that an intra-abdominal bowel distention of ≥10 mm between 20 and 22 weeks of gestation is predictive of complex gastroschisis with a specificity of 100%, a positive predictive value of 100%, and a negative predictive value of 77%.[6]

The goal of treatment for simple gastroschisis is primary reduction of the herniated viscera. Delays in reduction increase the risk of visceral injury and the development of abdominal compartment syndrome (persistent intra-abdominal pressure [IAP] > 20 mm Hg). Staged reduction, usually with the use of a spring-loaded silo, is the preferred method to decrease IAP and lessen the risk of complications with primary reduction. Ultimately, the closure may be sutured, which is associated with a high risk of infection, or sutureless closure, which can be performed at the bedside, but is associated with a high rate of secondary hernia. Postoperatively, the infant is

advanced to full feedings, with a return of bowel function typically occurring within 4 weeks.[7]

The treatment of complex gastroschisis is often intensive and must be individualized depending on patient comorbidities, time of delivery, and the proportion of herniated viscera to abdominal domain. Intestinal perforation or necrosis is addressed at the time of surgical exploration and reduction; primary resection and anastomosis are often feasible. Resections should be minimal to avoid the development of short-gut syndrome, and ostomies are usually avoidable.[7]

Common to both simple and complex gastroschisis, the complications include abdominal compartment syndrome, NEC, midgut volvulus, and adhesive small bowel obstruction. Abdominal compartment syndrome is defined as persistent IAP (> 20 mm Hg), which leads to organ dysfunction, including anuria. NEC develops in 5-20% of patients, is usually mild, and infrequently requires surgical intervention. Midgut volvulus develops in approximately 1.2% of patients due to adhesion of the small bowel to the lateral abdominal wall. Adhesive small bowel obstruction is reported in 20-25% of patients, usually within the first year of life. In addition to these complications, outcomes differ significantly between simple and complex gastroschisis. Complex cases generally have a prolonged recovery, with a medical hospital stay of 75.4 days and time to full enteral feeding of 58.1 days, compared with 35.1 days and 24.1 days, respectively, for simple gastroschisis.[8] This disparity highlights the greater burden of care and higher risk of complications in complex gastroschisis, likely due to increased IAP and fascia closure tension, which can result in organ dysfunction, bowel inflammation, and adhesions.[7] Most infants with simple gastroschisis live a normal lifespan, while those with complex gastroschisis have more complications that can increase morbidity and mortality.

Conclusion

An external protrusion of the intestines and occasionally other organs without a protective membrane is the hallmark of gastroschisis. Prenatal US, specifically the marker IABD, is the most effective in diagnosing and differentiating between simple and complex gastroschisis. Patients diagnosed with the condition are at a risk of infection, sepsis, and electrolyte imbalances from swelling and inflammation of the exposed organs. Treatment aims for primary reduction of the herniated viscera to prevent visceral injury and abdominal compartment syndrome. Staged reduction using a spring-loaded silo is the preferred method. Complex cases should be treated individually, and any resection should be kept to a minimum to prevent short-gut syndrome. Reported complications include abdominal compartment syndrome (up to 25%), NEC (5%), midgut volvulus (1.2%), and adhesive small bowel obstruction (20-25%).

References

1) Fatona O, Opashola K, Faleye A, et al. Gastroschisis in Sub-Saharan Africa: a scoping review of the prevalence, management practices, and associated outcomes. *Pediatr Surg Int*. 2023;39(1):246. doi:10.1007/s00383-023-05531-w

2) Bhat V, Moront M, Bhandari V. Gastroschisis: a state-of-the-art review. *Children*. 2020;7(12):302. doi:10.3390/children7120302

3) Bence CM, Wagner AJ. Abdominal wall defects. *Transl Pediatr*. 2021;10(5):1461-1469. doi:10.21037/tp-20-94

4) Muniz TD, Rolo LC, Araujo Júnior E. Gastroschisis: embriology, pathogenesis, risk factors, prognosis, and ultrasonographic markers for adverse neonatal outcomes. *J Ultrasound*. 2024;27(2):241-250. doi:10.1007/s40477-024-00887-8

5) Rentea RM, Gupta GV. Gastroschisis; 2020. https://www.ncbi.nlm.nih.gov/books/NBK557894/

6) Joyeux L, Belfort MA, Coppi P, et al. Complex gastroschisis: a new indication for fetal surgery. *Ultrasound Obstet Gynecol*. 2021;58(6):804-812. doi:10.1002/uodg.24759

7) Bielicki IN, Somme S, Frongia G, Holland-Cunz SG, Vuille-dit-Bille RN. Abdominal wall defects—current treatments. *Children*. 2021;8(2):170. doi:10.3390/children80201704

8) Jaczyńska R, Mydlak D, Mikulska B, et al. Perinatal outcomes of neonates with complex and simple gastroschisis after planned preterm delivery-a single-centre retrospective cohort study. *Diagnostics*. 2023;13(13):2225. doi:10.3390/diagnostics13132225

Congenital Nasal Pyriform Aperture Stenosis

Amin Lim, BA; Richard B. Towbin, MD; Carrie M. Schaefer, MD; Alexander J. Towbin, MD

Abstract

Patients with congenital nasal pyriform aperture stenosis typically present with respiratory distress, including noisy breathing resembling snoring, apneic episodes during wakefulness and sleep, feeding difficulties, and failure to thrive. Sudden airway obstruction may occur but can be temporarily relieved by crying. Imaging plays a key role in diagnosis, with a pyriform aperture width of <11 mm considered diagnostic. While surgical intervention can be curative, the timing of surgery should be individualized based on symptom severity and overall prognosis. Supportive care remains essential to optimize outcomes and ensure the best possible management approach.

Keywords: head and neck, nose, congenital

Case Summary

A 4-week-old child presented with nasal obstruction and feeding difficulties.

Imaging Findings

Axial CT showed narrowing of the pyriform aperture, with the bony aperture measuring <4.5 mm in width with a high degree of obstruction (Figure 1). There were paired central incisors and a normal pituitary fossa and gland (not shown).

Diagnosis

Congenital nasal pyriform aperture stenosis.

The clinical differential diagnosis of neonatal nasal obstruction includes choanal atresia, nasopharyngeal encephalocele, mucosal edema, dermoid cysts, skull base malformations, tumors, nasal hypoplasia, and nasal trauma.

Discussion

Congenital nasal pyriform aperture stenosis, also referred to as nasal inlet stenosis, is a rare cause of neonatal respiratory distress, with an estimated prevalence of 1 in 25,000 live births.[1] The condition is thought to result from excessive growth of the nasal process of the maxilla, leading to a narrowing of the pear-shaped pyriform aperture and increased airway resistance.[2] This anatomical narrowing restricts airflow, making it difficult for neonates to breathe.[3] Because newborns are obligate nasal breathers, severe nasal obstruction can lead to life-threatening respiratory distress.[4]

Neonates with congenital nasal pyriform aperture stenosis typically present with respiratory distress, noisy breathing resembling snoring, and episodes of apnea both during wakefulness and sleep. Additional symptoms include feeding difficulties, failure to thrive, and sudden airway obstruction, which may be temporarily relieved by crying.[5] The timing of symptom onset depends on the severity of the stenosis, with signs appearing as early as the first hours of life or developing months later.

Figure 1. Axial CT at the level of the nasal cavity showing severe narrowing (arrow) of both nasal pyriform apertures measuring <4.5 mm in width with a high degree of obstruction. There were paired central incisors and a normal pituitary fossa and gland (not shown).

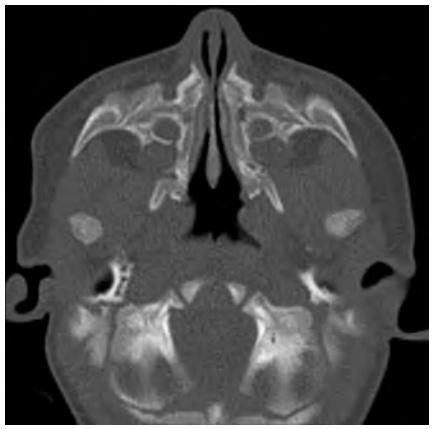

While the exact pathology of congenital nasal pyriform aperture stenosis remains unclear, the condition has been associated with several genetic syndromes. Documented links exist between congenital nasal pyriform aperture stenosis and

Affiliations: University of Texas Medical Branch John Sealy School of Medicin, Galveston, Texas (Lim); Department of Radiology, Phoenix Children's Hospital, Phoenix, Arizona (RB Towbin, Schaefer); Department of Radiology, Cincinnati Children's Hospital, University of Cincinnati College of Medicine, Cincinnati, Ohio (AJ Towbin).

Disclosures: The authors have no conflicts of interest to disclose. None of the authors received outside funding for the production of this original manuscript and no part of this article has been previously published elsewhere.

https://doi.org/10.37549/JPCR-26-0100

semi lobar holoprosencephaly, craniofacial anomalies, solitary median maxillary central incisor, and endocrinologic disorders such as hypopituitary axis abnormalities.[4]

Although awareness of congenital nasal pyriform aperture stenosis has increased in recent years, its rarity and variable presentation continue to pose diagnostic challenges.[4] Distinguishing it from other causes of nasal obstruction requires a combination of clinical examination and maxillofacial CT findings. According to Baker and Pereira, suggestive physical examination findings include a narrowed anterior nasal fossa and the inability to pass a 5-French catheter or a 1.9-mm endoscope through the nasal cavity.[3]

Definitive diagnosis of congenital nasal pyriform aperture stenosis is established using thin-section CT imaging of the nose and face, which directly visualizes the stenotic pyriform aperture.[4] Maxillofacial CT should be performed in a plane parallel to the hard palate using 1.5-2-mm axial sections to accurately measure the dimensions of the pyriform aperture.[4] A pyriform aperture width of <11 mm in a term infant is considered diagnostic.

Beyond confirming the diagnosis, maxillofacial CT is essential for evaluating the severity of obstruction, identifying associated anomalies, and assessing the surrounding bony architecture.[4] In cases where comorbid conditions with a poor prognosis are suspected, additional imaging, such as a CT or US of the brain, should be performed before considering surgical intervention.[4]

The treatment of congenital nasal pyriform aperture stenosis depends on the severity of symptoms, the degree of airway obstruction, and the overall prognosis of the infant.[4] Initial management involves the use of a McGovern nipple or oral airway, along with supportive care such as nasal humidification, suctioning, topical steroids, and decongestant drops.[6] In infants with multiple anomalies and a poor prognosis, conservative management is typically recommended, with prognosis assessed based on comorbidities that contribute to failure to thrive.

Surgical treatment is reserved for infants with severe nasal obstruction who have a good prognosis and no significant comorbidities, or for those in whom 2 weeks of aggressive medical therapy has failed.[7] The "rule of 10" is often applied to determine optimal surgical timing, recommending deferral until the infant reaches 10 pounds, 10 weeks of age, and a hemoglobin level of 10 g/dL, provided that the child's respiratory status remains stable.[7] Until these criteria are met, supportive care should continue to optimize surgical outcomes.

Conclusion

Patients with congenital nasal pyriform aperture stenosis typically present with respiratory distress, including noisy breathing resembling snoring, apneic episodes during wakefulness and sleep, feeding difficulties, and failure to thrive. Sudden airway obstruction may occur but can be temporarily relieved by crying. Imaging plays a key role in diagnosis, with a pyriform aperture width of <11 mm considered diagnostic. While surgical intervention can be curative, the timing of surgery should be individualized based on symptom severity and overall prognosis. Supportive care remains essential to optimize outcomes and ensure the best possible management approach.

References

1) Tropsek R, Horoi M, Ziereisen F. Congenital nasal pyriform aperture stenosis in association with polymalformative syndrome of the midline. *Cureus*. 2023;15(9):e45153. doi:10.7759/cureus.45153

2) Brown OE, Myer CM 3rd, Manning SC. Congenital nasal pyriform aperture stenosis. *Laryngoscope*. 1989;99(1):86-91. doi:10.1288/00005537-198901000-00016

3) Ey EH, Han BK, Towbin RB, Jaun WK. Bony inlet stenosis as a cause of nasal airway obstruction. *Radiology*. 1988;168(2):477-479. doi:10.1148/radiology.168.2.3393667

4) Baker KA, Pereira KD. Congenital nasal pyriform aperture stenosis. *Oper Tech Otolaryngol Head Neck Surg*. 2009;20(3):178-182. doi:10.1016/j.otot.2009.11.001

5) Serrano TLI, Pfeilsticker L, Silva V, et al. Newborn nasal obstruction due to congenital nasal pyriform aperture stenosis. *Allergy Rhinol*. 2016;7(1):e37-e41. doi:10.2500/ar.2016.7.0146

6) Shikowitz MJ. Congenital nasal pyriform aperture stenosis: diagnosis and treatment. *Int J Pediatr Otorhinolaryngol*. 2003;67(6):635-639. doi:10.1016/s0165-5876(03)00018-1

7) Hui Y, Friedberg J, Crysdale WS. Congenital nasal pyriform aperture stenosis as a presenting feature of holoprosencephaly. *Int J Pediatr Otorhinolaryngol*. 1995;31(2):263-274. doi:10.1016/0165-5876(94)01096-g

8) Van Den Abbeele T, Triglia J-M, François M, Narcy P. Congenital nasal pyriform aperture stenosis: diagnosis and management of 20 cases. *Ann Otol Rhinol Laryngol*. 2001;110(1):70-75. doi:10.1177/000348940111000113

9) Marrugo Pardo GE, Parra Charris JS, Parra Charris AE, Villa Zuluaga DF. Congenital nasal pyriform aperture stenosis: diagnosis, management and technical considerations. *Acta Otorrinolaringologica*. 2020;71(3):154-159. doi:10.1016/j.otoeng.2020.02.001

Atrial Septal Defect

Rose Kalu Igwe, BS; Richard B. Towbin, MD; Jason N. Johnson, MD; Alexander J. Towbin, MD

Abstract

Atrial septal defects (ASDs) represent a significant congenital heart condition with the potential for severe long-term complications if left untreated. Imaging advances, particularly modalities such as transthoracic echocardiography, cardiac CT, and cardiac MRI, have greatly enhanced the early detection and precise characterization of ASD, allowing for more effective and personalized treatment strategies. These tools not only aid in distinguishing the type and severity of the defect but also provide invaluable guidance for surgical interventions, thereby improving patient outcomes.

Keywords: thorax, cardiac, congenital, shunt

Case Summary

A teenage female presented with worsening fatigue and shortness of breath with physical activity. Her physical exam showed a fixed split-second heart sound and a systolic ejection murmur of the left upper sternal border.

Imaging Findings

Transthoracic echocardiogram (Figure 1) showed a large secundum atrial septal defect (ASD) with left to right shunting and moderate right atrial and ventricular dilation. The cardiac MRI (Figure 2) confirmed the large secundum ASD, moderate right atrial and ventricular chamber dilation, normal pulmonary venous anatomy, and an increased Qp:Qs.

Diagnosis

Atrial septal defect.

Figure 1. (A) Parasternal short-axis transthoracic echocardiogram at end-diastole showing moderate right ventricular chamber dilation. MV, mitral valve; RV, right ventricle. (B) Subcostal coronal color compare at end-diastole showing a large secundum ASD. ASD, atrial septal defect; LA, left atrium; RA, right atrium.

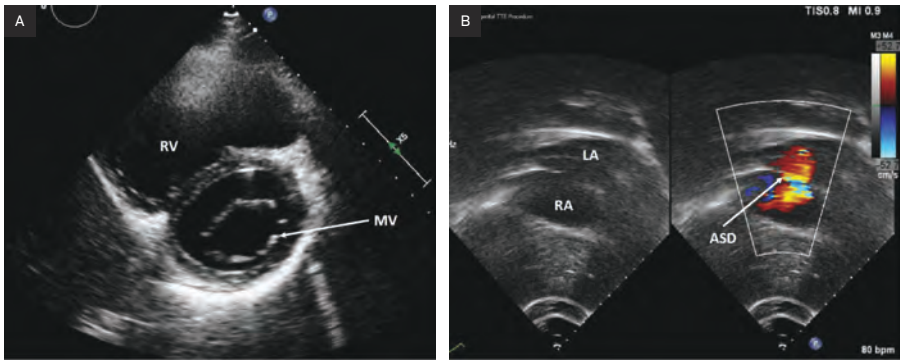

The differential diagnosis for ASD in childhood includes atrioventricular septal defect, total anomalous pulmonary venous return, pulmonary stenosis, and ventricular septal defect.

Discussion

ASD is the second most common congenital heart defect in childhood after ventricular septal defect. ASD occurs in 0.2% of children or 1-2 per 1000 births.[1] In the past 60 years, the rate of ASDs has risen from below 0.5 cases per 1000 live births to around 1.6 per 1000.[1] This increase in prevalence is due to the improvement of imaging modalities and improved clinical detection due to educational and technical advancements of medical practitioners.[1] An ASD is defined as an abnormal opening in the interatrial septum, which leads to blood shunting between the atria.[1] Generally, small ASDs close on their own. However, larger ASDs cause cardiac and respiratory issues into adulthood.[1] ASD is more common in girls than boys, with a male-to-female ratio of 1:2, and is influenced by specific genetic conditions.[1]

Affiliations: A.T Still University- Kirksville College of Osteopathic Medicine, Kirksville, Missouri (Igwe); Department of Radiology, Phoenix Children's Hospital, Phoenix, Arizona (RB Towbin); Heart Institute, Le Bonheur Children's Hospital, Memphis, Tennessee (Johnson); Department of Radiology, Cincinnati Children's Hospital and University of Cincinnati College of Medicine, Cincinnati, Ohio (AJ Towbin).
Disclosures: The authors have no conflicts of interest to disclose. None of the authors received outside funding for the production of this original manuscript and no part of this article has been previously published elsewhere.

https://doi.org/10.37549/JPCR-26-0101

Figure 2. (A) A 4-chamber CMR cine steady state free precession (SSFP) at end-diastole showing a large secundum ASD (yellow asterisk), moderately dilated right atrium and right ventricle, and a small anterior pericardial effusion. The right ventricular end-diastolic volume was 120 mL/m^2 (normal 60-100 mL/m^2). LA, left atrium; LV, left ventricle; RA, right atrium; RV, right ventricle. (B) ASD en face view (off-axis coronal view) CMR cine SSFP at end-diastole showing a large secundum ASD (yellow arrow). ASD, atrial septal defect; LV, left ventricle; RV, right ventricle; SVC, superior vena cava. (C). ASD en face view CMR phase contrast through plane at end-diastole showing the shunting through the ASD (yellow arrow). The flow through the ASD was 4.59 L/minute. The flow across the aortic valve was 3 L/minute, and the pulmonary valve was 7.60 L/minute. The calculated Qp:Qs was 2.5:1. ASD, atrial septal defect.

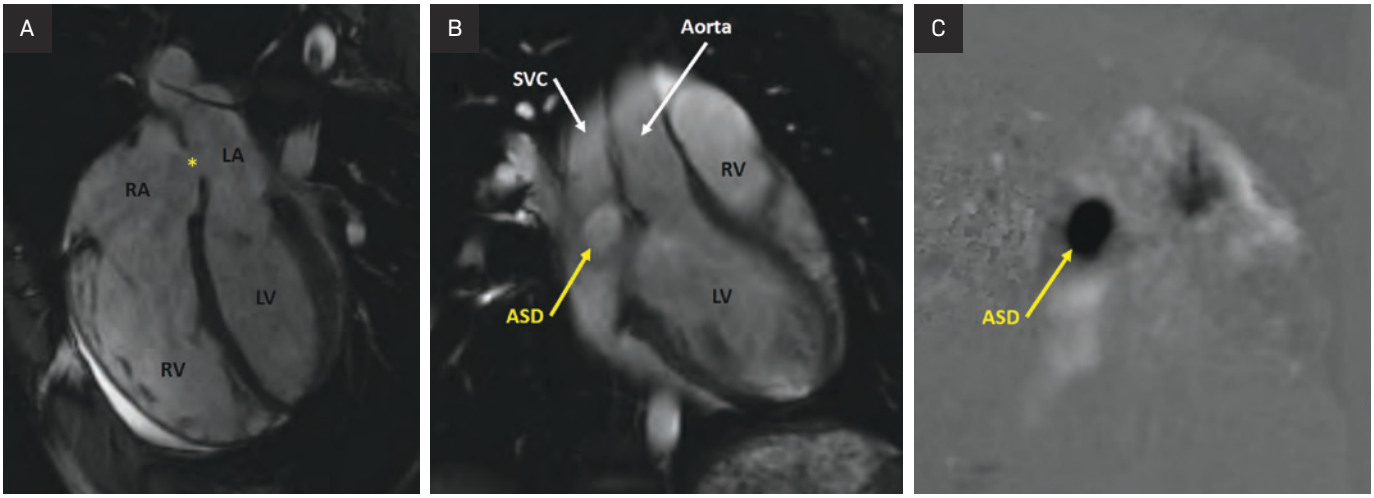

A variety of syndromes are associated with ASDs as well as other congenital cardiac defects. Holt-Oram syndrome, caused by mutations in the TBX5 gene, affects heart and upper limb development.[1,2] Ellis-van Creveld syndrome, due to mutations in the EVC or EVC2 genes, is strongly associated with dysrhythmias and secundum ASDs and more common in certain Amish and Indigenous Australian communities.[1] In addition to ASDs, patients with this syndrome commonly present with a single atrium.[1] Some families also show a pattern of ASDs linked to mutations in the NKX2.5 and GATA4 genes, emphasizing the complex genetic factors that can contribute to this condition.[1] These associations are heavily influenced by Mendelian inheritance and maternal exposure to alcohol, drugs like cocaine, and rubella.[1]

ASDs involve a true septal deficiency that promotes communication of blood between the atria of the heart.[1] In a normal heart, the interatrial septum separates the right and left atria, preventing oxygenated and deoxygenated blood from mixing.[3] Structurally, the interatrial septum includes the septum primum and septum secundum, which develop during embryogenesis to fully divide the atria.[3] The septum primum begins as a thin membrane growing from the upper part of the common atrium downward, closing the initial opening between the left and right sides.[3] The septum secundum then forms on the right side, partially covering a secondary opening and creating the fossa ovalis, which allows prenatal blood flow between the atria.[3] Proper septal formation allows for appropriate separation of the circulation and oxygen-poor blood to flow into the right atrium and oxygen-rich blood to enter the left atrium.[3] ASDs disrupt this structure by creating openings in the septum that permit abnormal shunting of blood between the atria.[3] Pathologically, these defects typically lead to increased blood flow in the right atrium and ventricle in patients without pulmonary hypertension and normal right ventricular compliance because they create a left-to-right shunt, allowing oxygen-rich blood from the left atrium to flow back into the right atrium.[3] This added volume causes the right heart to enlarge as it accommodates the extra workload.[3] Additionally, the increased blood flow to the lungs raises both blood volume and pressure in the pulmonary circulation, further stressing the right side of the heart and pulmonary vessels.[3]

There are 4 types of ASD: including a secundum ASD, primum ASD, sinus venosus, and unroofed coronary sinus.[3] Secundum ASD makes up 75% of ASD cases and is characterized by a large fossa ovalis or deficient septum primum. It is usually located in the central part of the septum due to increased reabsorption of the septum primum or the septum secundum fails to occlude the ostium secundum.[2] Primum ASD makes up 15-20% of ASD cases and is located at the lower region of the septum because they arise from improper formation of the septum primum and endocardial cushions, which are essential for dividing the atria and ventricles.[1] Primum ASD is often a part of an atrioventricular canal defect and is usually associated with trisomy 21.[2] Sinus venous defect makes up <10% of ASD cases and is usually associated with atypical drainage of the right superior or inferior pulmonary vein into the superior vena cava or inferior vena cava (partial anomalous pulmonary venous return).[1] Lastly, an unroofed coronary sinus, otherwise known as coronary sinus ASD, arises due to maldevelopment in

the wall separating the coronary sinus and left atrium.[3] A notable mention is patent foramen ovale.[3] It occurs when the opening between the right and left atria that is normally present in fetal circulation (fossa ovalis) fails to close after birth.[3] The patent foramen ovale typically closes shortly after birth and is not considered an ASD because no septal tissue is missing.[3]

Clinical appearances of ASDs in children depend on their age, the size of the shunt, and the presence or absence of mitral incompetence.[1] Small ASDs, usually <6 mm in size, are likely to close spontaneously, with closure occurring in 89% of cases for 4-mm defects and 79% for 5-6-mm defects, often within the first year of life.[4] In contrast, defects larger than 8 mm have only a 4% chance of spontaneous closure, with 91% requiring surgical or catheter-based intervention.[2,4] Without intervention, larger ASDs lead to a left-to-right shunt that increases blood flow to the right heart and lungs as long as the pulmonary vascular resistance (PVR) remains low.[4] This overload can cause cardiomegaly, pulmonary plethora, and right ventricular dilation and ultimately hypertrophy, as well as elevated pressures in the pulmonary arteries, leading to pulmonary hypertension.[4] Over time, these effects can also dilate the proximal pulmonary arteries, underscoring the need for timely treatment.[1] In patients with long-standing large ASDs without treatment that develop pulmonary hypertension, the shunting across the ASD becomes right to left and patients develop desaturations.

Imaging plays a major role in the diagnosis, size determination, and course of treatment of ASD.[5] The gold standard for diagnostic imaging for children and adults is the echocardiogram.[5] The transthoracic echocardiography (TTE) is the preferred imaging method for diagnosing ASDs in children due to its noninvasive nature, accessibility, and clear visualization of cardiac structures.[5] It examines the blood flow direction via color Doppler imaging, pressure of the pulmonary artery (PA), size of opening, systemic and pulmonary flow ratio, and to uncover other associated abnormalities.[1] It effectively evaluates the defect's size, location, and any impacts on the heart, especially in younger children who typically provide good imaging windows.[5] However, as children grow older or if more detailed imaging is required for procedures like transcatheter closure, transesophageal echocardiography (TEE) becomes more advantageous.[5] TEE offers superior detail of the septal region and surrounding structures, making it valuable for complex cases or older patients.[5] Thus, age plays a role in choosing the most suitable imaging technique. Other imaging tools that could be used are cardiac CT scan, MRI, catheter angiography, and chest x-ray.

A CT scan provides detailed visualization of the wall thickness and chamber diameter.[1] It could also be used to measure the aortopulmonary ratio of the patient. Cardiac MRI allows for the quantification of the pulmonary blood flow (Qp) to systemic blood flow (Qs) ratio (Qp:Qs), stroke volume, right ventricular volume, and atrial level shunt.[1] Its high spatial resolution allows for precise measurement of the ASD, a critical factor in guiding clinical decision-making and optimizing therapeutic interventions for pediatric patients.[1] Cardiac MRI can be used to calculate the flow across the ASD to help confirm the amount of shunting through the defect, and the flow across the ASD plus the flow across the aortic valve will equal the flow across the pulmonary valve (Qs + QASD = Qp). Catheter angiography is typically employed when assessing older patients or when pressure measures are needed to assess for evidence of pulmonary hypertension.[1] Chest x-rays can also be used to observe clinical status via the identification of enlargement in the heart and PA.[2]

In pediatric patients with ASD, treatment options primarily include transcatheter closure and surgical repair, chosen based on defect characteristics and size, patient age, and overall health. Transcatheter closure is often the preferred method for secundum ASDs in children due to its minimally invasive nature and high success rate in defects up to 35 mm in diameter.[6] To minimize procedural risks, transcatheter closure is usually recommended for patients weighing over 15 kg, with thresholds such as a systolic PA pressure <50% systemic and a PVR below one-third of systemic vascular resistance.[6] This approach has shown success rates exceeding 95%, with benefits including shorter recovery times and reduced hospital stays.[6] However, risks in younger patients may include vascular complications and rare device embolization, mitigated with meticulous pre-procedure imaging.[6]

Surgical repair is typically reserved for larger, complex ASDs or non-secundum defects, such as primum or sinus venosus types, which present anatomical challenges unsuitable for device closure. This method, which also requires careful consideration of PA pressure and PVR thresholds, carries the inherent risks associated with cardiopulmonary bypass, such as infection and bleeding, though it remains effective with low recurrence rates.[6] Given the diversity of device options for transcatheter closure, including the Amplatzer Septal Occluder (Abbott Laboratories, Chicago, Illinois, USA) and Gore Cardioform Occluder (Gore, Newark, Delaware, USA), echocardiography is used to assess defect size and positioning, aiding in device selection and minimizing procedural complications.[6] In pediatric ASD management, both treatment approaches yield high efficacy with careful threshold-based risk management, ensuring successful outcomes with personalized care for each child's specific needs.[6] For patients with ASD who are symptomatic or not immediately eligible for surgery, medical management is essential. Anticoagulants help reduce the risk of clot formation, beta-blockers manage irregular heart

https://doi.org/10.37549/JPCR-26-0101

rhythms, and diuretics help alleviate fluid accumulation.[7] In pediatrics, early detection through prenatal care and advanced imaging, like TTE, plays a critical role in identifying ASDs early, allowing for timely intervention.[7] Together, these medical strategies and diagnostic tools improve outcomes by addressing symptoms and preventing complications until or if surgery becomes viable.

Conclusion

ASDs represent a significant congenital heart condition with the potential for severe long-term complications if left untreated. Imaging advances, particularly modalities such as TTE, cardiac CT, and cardiac MRI have greatly enhanced the early detection and precise characterization of ASD, allowing for more effective and personalized treatment strategies. These tools not only aid in distinguishing the type and severity of the defect but also provide invaluable guidance for surgical interventions, thereby improving patient outcomes.

References

1) Feger J. Atrial septal defect. Radiopaedia. https://radiopaedia.org/articles/atrial-septal-defect-2?lang=us#references

2) Menillo AM, Lee L, Pearson-Shaver AL. Atrial septal defect (ASD). Nih.gov; 2023. https://www.ncbi.nlm.nih.gov/books/NBK535440/

3) Bartoszewska E, Chrapkowska A, Zielińska O, et al. Atrial septal defects: from embryology to pediatric pulmonary hypertension. *J Clin Med*. 2025;20(3):7698. doi:10.1007/s002469900439

4) Helgason H, Jonsdottir G. Spontaneous closure of atrial septal defects. *Pediatric Cardiology*. 1999;20(3):195-199. doi:10.1007/s002469900439

5) Deri A, English K. Echocardiographic assessment of left to right shunts: atrial septal defect, ventricular septal defect, atrioventricular septal defect, patent arterial duct. *Echo Res Pract*. 2018;5(1):R1-R16. doi:10.1530/ERP-17-0062

6) Turner ME, Bouhout I, Petit CJ, Kalfa D. Transcatheter closure of atrial and ventricular septal defects: jacc focus seminar. *J Am Coll Cardiol*. 2022;79(22):2247-2258. doi:10.1016/j.jacc.2021.08.082

7) Stout KK, Daniels CJ, Aboulhosn JA, et al. 2018 AHA/ACC guideline for the management of adults with congenital heart disease: a report of the American college of cardiology/American heart association task force on clinical practice guidelines. *Circulation*. 2019;139(14):e698-e800. doi:10.1161/CIR.0000000000000603